

## Characteristics of large electric-dipole moment states in crossed electric and magnetic fields studied by quantum calculations

Sihong Gu,\* Wenyu Liu, and Shunsheng Gong

Laboratory of Magnetic Resonance and Atomic and Molecular Physics, Wuhan Institute of Physics, The Chinese Academy of Sciences, Wuhan 430071, People's Republic of China

Baiwen Li

Chinese Center of Advanced Science and Technology (World Laboratory), P.O. Box 8730, Beijing, People's Republic of China and Wuhan Institute of Physics, The Chinese Academy of Sciences, Wuhan 430071, People's Republic of China

(Received 2 December 1996)

Using a matrix diagonalization method, atomic Rydberg states with large electric-dipole moment states in strong crossed electric and magnetic fields with  $\epsilon=0.075$  ( $\epsilon=EB^{-4/3}$ ; we use atomic units) are studied. The characteristics of the states and the influence of the atomic core on the large electric-dipole moment states are discussed. [S1050-2947(97)09507-3]

PACS number(s): 32.60.+i

### I. INTRODUCTION

Rydberg-atomic behavior in strong crossed electric and magnetic fields is an interesting subject. In addition to the usual aspects of the problem associated with fields and atoms, this subject also has its own characteristics. One is the possible existence of bound states corresponding to the second potential well that is formed by crossed electric and magnetic fields, and the other is the condition for the electron motion to become chaotic.

There have been many theoretical results on the subject of strong crossed fields [1,2] and some progress has also been made in experimental studies. With rubidium Rydberg atoms Fauth *et al.* carried out the experiments to detect the bound states corresponding to the second potential well [3]; Wiebusch *et al.* studied classical chaos and bound states related to the second well through the analysis of their experimental spectra of highly excited hydrogen atoms in strong crossed fields [4]. In recent years Raithel *et al.* have made a series of interesting advances in the case of strong magnetic field combined with the different strength of crossed electric fields. One of these is that with a relatively weak electric field  $\epsilon < 0.1$  ( $\epsilon=EB^{-4/3}$  is the scaled electric field in atomic units) they observed large electric-dipole moment states. In addition to this interesting experimental result, they also made theoretical discussions in light of semiclassical analysis and came to some conclusions regarding the features of large electric-dipole moment states, and characteristics of  $\langle l_z \rangle$ ,  $\langle l_z \rangle^2 - \langle l_z^2 \rangle$ , etc. were obtained from the analysis [5]. These theoretical studies are helpful in recognizing the characters of these states.

However, to our knowledge, there have not been studies of these states based on quantum-mechanical calculations. Such quantum mechanical studies are of quantitative significance and they serve to verify and complement semiclassical studies. The quantitative aspects include the following: (1)

oscillator strengths that are not readily available in semiclassical studies; (2) the conclusions about some quantum mechanical quantities such as  $\langle l_z \rangle$ ,  $\langle l_z \rangle^2 - \langle l_z^2 \rangle$  related to large electric-dipole moment states, which are obtained in the light of correspondence, are open to verifications by means of quantum calculations; (3) the complication due to the atomic core of the alkali-metal atom used in experiments can only be handled with quantum-mechanical calculations. Based on these considerations we study these large electric-dipole moment states through quantum-mechanical calculations using a matrix diagonalization method.

### II. CALCULATION METHOD

The alkali-metal atom of our interest is sodium and to illustrate the atomic core effect and to compare with semiclassical results we also make calculations for the hydrogen atom.

Generally the total core effect is described by the quantum defect  $\delta_{nl}$  [6]. For Na the quantum defects of *S* and *P* states are about 1.35 and 0.88, respectively. In the calculations for Na we choose as our basis functions the zero-field potential model [7]. Considering the penetration and polarization effects, the core potential is assumed to be dependent on the principal quantum number *n* and angular quantum number *l* and takes the form

$$V(r) = -\frac{1}{r} \left( 1 + \frac{\beta'}{(r+\gamma')^2} + \frac{\kappa'}{(r+\xi')^2} \right). \quad (1)$$

Due to the spherical symmetry of the potential, the wave function in zero field has the following form:

$$\Psi_{nlm} = R_{nl}(r) Y_{lm}(\theta, \varphi), \quad (2)$$

where *n*, *l*, and *m* are principal, angular, and magnetic quantum numbers, respectively,  $Y_{lm}(\theta, \varphi)$  is a spherical harmonic, and  $R_{nl}(r)$  has an analytic form,

\*Electronic address: dsguo@cluster.engr.subr.edu

TABLE I. H atom, even  $\pi_z$  parity, large  $d_s$  states, excited from  $1S$  with laser polarization along  $\mathbf{E}$ .  $W$  is the state energy,  $D(l_z)$  is  $\langle l_z^2 \rangle - \langle l_z \rangle^2$ , and  $w$  is the component of the corresponding zero-field state.  $W$ ,  $\langle x \rangle$ , and  $d_s$  are in atomic units. All states with main components  $8 \leq n \leq 11$ ,  $|d_s| > 0.1$ , and  $W$  in the range  $(-0.0093, -0.0032)$  a.u., that is,  $(-2040, -700) \text{ cm}^{-1}$  are listed in the table. The quantum numbers of zero-field states with components ( $w$ )  $> 0.1$  are listed. The numbers in brackets represent powers of 10.

$W$	$f$	$\langle l_z \rangle$	$D(l_z)$	$\langle x \rangle$	$d_s$	$m$	$l$	$n$	$w$
-0.92132626[-2]	0.190[-14]	-7.0	0.05	-12	-0.108	-7	7	8	0.95
-0.77350031[-2]	0.498[-16]	-7.9	0.07	-17	-0.131	-8	8	9	0.93
-0.74822488[-2]	0.419[-13]	-6.9	0.19	-15	-0.115	-7	7	9	0.82
						-6	6	9	0.10
-0.73391752[-2]	0.953[-13]	-6.0	0.06	-14	-0.101	-6	8	9	0.94
-0.67060409[-2]	0.121[-17]	-8.9	0.10	-23	-0.156	-9	9	10	0.90
-0.64399801[-2]	0.118[-14]	-7.9	0.23	-21	-0.138	-8	8	10	0.78
						-7	7	10	0.12
-0.63205542[-2]	0.250[-14]	-7.0	0.09	-20	-0.126	-7	9	10	0.91
-0.61795945[-2]	0.431[-12]	-6.9	0.37	-20	-0.121	-8	8	10	0.10
						-7	7	10	0.67
						-6	6	10	0.16
-0.60712269[-2]	0.142[-11]	-6.0	0.21	-18	-0.108	-6	8	10	0.79
						-5	7	10	0.10
-0.59632202[-2]	0.247[-19]	-10	0.16	-31	-0.184	-10	10	11	0.84
-0.59249861[-2]	0.744[-10]	-5.9	0.49	-18	-0.105	-7	7	10	0.14
						-6	6	10	0.56
						-5	5	10	0.20
-0.56829069[-2]	0.283[-16]	-9.0	0.30	-29	-0.163	-9	9	11	0.71
						-8	8	11	0.13
-0.55892381[-2]	0.150[-17]	-8.0	0.15	-27	-0.153	-8	10	11	0.85
-0.54088167[-2]	0.130[-13]	-8.0	0.64	-27	-0.145	-8	8	11	0.58
						-7	7	11	0.17
-0.53284143[-2]	0.458[-13]	-7.0	0.27	-25	-0.132	-7	9	11	0.73
						-6	8	11	0.12
-0.52057438[-2]	0.164[-12]	-6.0	0.13	-23	-0.122	-6	10	11	0.85
-0.51411336[-2]	0.296[-11]	-6.9	0.59	-24	-0.126	-8	8	11	0.12
						-7	7	11	0.48
						-6	6	11	0.21
-0.50731857[-2]	0.110[-10]	-6.0	0.40	-22	-0.114	-6	8	11	0.60
						-5	7	11	0.15
-0.49660063[-2]	0.207[-09]	-5.0	0.24	-20	-0.100	-5	9	11	0.70
-0.48800384[-2]	0.352[-09]	-5.9	0.73	-22	-0.108	-7	7	11	0.16
						-6	6	11	0.39
						-5	5	11	0.24

$$R_{nl}(r) = N \exp(-\rho/2) \rho^s (\rho + \gamma)^t (\rho + \xi)^u \sum_{\nu=0}^{\infty} a_{\nu} \rho^{\nu}, \quad a_0 = 1, \quad (3)$$

$$\left[ -\frac{1}{r^2} \frac{d}{dr} \left( r^2 \frac{d}{dr} \right) + \frac{l(l+1)}{r^2} + V(r) \right] R_{nl}(r) = E_{nl} R_{nl}(r), \quad (5)$$

in which

$$\rho = \alpha r, \quad \gamma = \alpha \gamma', \quad \xi = \alpha \xi', \quad \alpha = 2/n^*, \quad n^* = n - \delta_{nl}, \quad (4)$$

where  $s, t, u, \alpha, \gamma', \xi', \kappa'$ , which depend on  $n$  and  $l$ , are the parameters to be determined, and  $\delta_{nl}$  is quantum defect. Substituting  $R_{nl}(r)$  and  $V(r)$  into the radial Schrödinger equation,

and then equating the coefficients of the corresponding terms of  $\rho$  and considering the asymptotic behavior and the standard condition for a radial wavefunction, we obtain the nonlinear algebraic equations of the above parameters. Solving them, we get  $R_{nl}(r)$  and  $V(r)$  in their analytic forms, where the sole input parameter  $\delta_{nl}$  can be determined by experiments. This radial wave function has the correct number of nodes, does not diverge in the origin of coordinates. Moreover, it has a behavior close to that of  $H-F-S$  wave function.

In the calculations of Na, the fine-structure interaction is

TABLE II. H atom, odd  $\pi_z$  parity, large  $d_s$  states, excited from 1S with laser polarization along  $\mathbf{B}$ . See Table I caption for details.

$W$	$f$	$\langle l_z \rangle$	$D(l_z)$	$\langle x \rangle$	$d_s$	$m$	$l$	$n$	$w$
-0.75379361[-2]	0.183[-16]	-7.0	0.07	-15	-0.116	-7	8	9	0.94
-0.65143397[-2]	0.437[-18]	-7.9	0.10	-22	-0.141	-8	9	10	0.91
-0.62565098[-2]	0.475[-15]	-6.9	0.22	-20	-0.123	-7	8	10	0.79
						-6	7	10	0.11
-0.61247832[-2]	0.379[-14]	-6.0	0.08	-18	-0.111	-6	9	10	0.90
-0.60040827[-2]	0.188[-12]	-5.9	0.34	-18	-0.106	-6	7	10	0.67
						-5	6	10	0.15
-0.57774926[-2]	0.568[-20]	-9.0	0.15	-29	-0.168	-9	10	11	0.85
-0.55068141[-2]	0.163[-16]	-8.0	0.29	-27	-0.148	-8	9	11	0.72
						-7	8	11	0.12
-0.53985976[-2]	0.125[-15]	-7.0	0.14	-25	-0.137	-7	10	11	0.86
-0.52421835[-2]	0.615[-14]	-6.9	0.42	-25	-0.129	-7	8	11	0.60
						-6	7	11	0.17
-0.51480154[-2]	0.729[-13]	-6.0	0.26	-23	-0.117	-6	9	11	0.73
						-5	8	11	0.11
-0.50109542[-2]	0.585[-12]	-5.0	0.12	-21	-0.106	-5	10	11	0.83
-0.49837603[-2]	0.146[-11]	-5.9	0.56	-22	-0.111	-7	8	11	0.12
						-6	7	11	0.49
						-5	6	11	0.20

eliminated. The Hamiltonian for both H and Na has the form of (in a.u.)

$$H = -\frac{1}{2}p^2 + V(r) + \frac{B}{2}L_z + \frac{B^2}{8}(x^2 + y^2) + E_x, \quad (6)$$

where the electric and magnetic fields are taken along the  $x$  and  $z$  axes, respectively; for the H atom  $V(r) = -1/r$  while for Na it is expressed by Eq. (1). In the crossed-fields case  $L_z$  does not commute with the Hamiltonian, but the parity operator with respect to the  $z=0$  plane,  $\Pi_z$  does, so that the eigenstates with  $l+m$  being even or odd correspond to even or odd parity ( $\pi_z = \pm 1$ ), respectively, and belong to different subspaces. In the calculations we take zero-field wavefunctions  $\Psi_{nlm}$  for the basis with even (odd)  $l+m$  for  $\pi_z = 1(-1)$  subspace. For even-parity subspace the number of total eigenvectors is  $\Sigma n(n+1)/2$  and for odd parity it is  $\Sigma n(n-1)/2$ . We choose  $B = 100$  T,  $E = 12400$  V/cm (corresponding to  $\epsilon \approx 0.075$ ), and a basis set  $3 < n < 17$  to make calculations for both H and Na. The range of interest is chosen near  $n = 10$  mainly for the consideration that the number of eigenvectors increases as  $n^3$ , which limits us to lower Rydberg states given our computer resources.

### III. RESULTS AND DISCUSSION

Tables I–IV list calculated results of the large electric-dipole moment states. These states are in the range  $(-2040, -700)$   $\text{cm}^{-1}$  and are mainly composed of  $nlm$  with  $8 \leq n \leq 11$ . Accuracy to the tabulated significant digits is guaranteed by checking the convergence behavior with an extended basis set ( $3 < n < 18$  for Na,  $2 < n < 18$  for H). With the enlarged basis set, the variations of the tabulated states are as follows: the energy differences are less than  $0.015$   $\text{cm}^{-1}$ , the relative differences of oscillator strengths,  $\langle l_z \rangle$ ,

$\langle l_z \rangle^2 - \langle l_z^2 \rangle$  and  $d_s$  ( $d_s = \langle x \rangle |W|$  is the scaled dipole moment, where  $\langle x \rangle$  is the expectation value of electric-dipole moment and  $W$  is the atomic energy) are less than 11%, 0.23%, 0.001%, and 0.15%, respectively. For those experimentally more observable states with oscillator strength  $> 10^{-7}$ , the variation of energy levels is less than  $0.006$   $\text{cm}^{-1}$ , the relative differences of transition probabilities,  $\langle l_z \rangle$ ,  $\langle l_z \rangle^2 - \langle l_z^2 \rangle$ , and  $d_s$  are less than 0.12%, 0.0078%, 0.0005%, and 0.088%, respectively.

Figures 1 and 2 show the relations between signal strengths and  $d_s$  of all states with energy levels in the range  $(-2040, -700)$   $\text{cm}^{-1}$ . The corresponding excitation process is from the ground state to high excited states with the polarization of the exciting laser parallel to the  $\mathbf{E}$  direction.

From Tables I and II one characteristic for the H atom is that the large  $d_s$  states all have a large  $|\langle l_z \rangle|$  value, which supports the conclusion by Raithel *et al.* From the viewpoint of quantum mechanics, the trajectories of high  $|\langle l_z \rangle|$  states are largely far away from the small  $r$  region, which is a characteristic of the drift states in semiclassical discussions [5]. It should also be noticed that  $\langle l_z \rangle$  and  $d_s$  of all large  $d_s$  states are negative. Another characteristic is that the oscillator strengths of the large  $d_s$  states are quite small, usually 7 orders of magnitude smaller than those of other states. From Tables III and IV it is seen that for Na the large  $d_s$  states can be classified into two groups. One is the hydrogen-like states that are found to correspond one-by-one to states of H in Tables I and II. The other is nonhydrogen states, which have the following characteristics: (1) large low- $l$  components and hence large oscillator strengths; (2) electric dipoles of the large  $d_s$  states can be either positive or negative, meaning that the wave function can be polarized either in or opposite to the direction of  $\mathbf{E}$ .

The excitation process of excitation of large  $d_s$  states is

TABLE III. Na atom, even  $\pi_z$  parity, large  $d_s$  states, exciting from  $3S$  with laser polarization along  $\mathbf{E}$ . See Table I caption for details.

$W$	$f$	$\langle l_z \rangle$	$D(l_z)$	$\langle x \rangle$	$d_s$	$m$	$l$	$n$	$w$
-0.92132626[-2]	0.796[-16]	-7.0	0.05	-12	-0.108	-7	7	8	0.95
-0.80488981[-2]	0.121[-06]	-2.1	0.33	13	0.106	-3	3	8	0.17
						-2	2	8	0.64
-0.77350031[-2]	0.900[-20]	-7.9	0.07	-17	-0.131	-8	8	9	0.93
-0.74822488[-2]	0.316[-13]	-6.9	0.19	-15	-0.115	-7	7	9	0.82
						-6	6	9	0.10
-0.73391753[-2]	0.757[-14]	-6.0	0.06	-14	-0.101	-6	8	9	0.94
-0.73300305[-2]	0.253[-06]	2.0	0.14	-14	-0.104	2	2	8	0.29
						2	4	8	0.21
						2	6	8	0.37
-0.73110745[-2]	0.558[-06]	1.9	0.21	-26	-0.194	1	1	9	0.11
						2	2	8	0.39
						2	6	8	0.40
-0.67060409[-2]	0.129[-19]	-8.9	0.10	-23	-0.156	-9	9	10	0.90
-0.64399801[-2]	0.899[-17]	-7.9	0.23	-21	-0.138	-8	8	10	0.78
						-7	7	10	0.12
-0.63205542[-2]	0.118[-16]	-7.0	0.09	-20	-0.126	-7	9	10	0.91
-0.61795948[-2]	0.521[-15]	-6.9	0.37	-20	-0.121	-8	8	10	0.10
						-7	7	10	0.67
						-6	6	10	0.16
-0.60712271[-2]	0.951[-15]	-6.0	0.21	-18	-0.108	-6	8	10	0.79
						-5	7	10	0.10
-0.59632202[-2]	0.131[-19]	-10	0.16	-31	-0.184	-10	10	11	0.84
-0.59249973[-2]	0.149[-14]	-5.9	0.50	-18	-0.105	-7	7	10	0.14
						-6	6	10	0.56
						-5	5	10	0.20
-0.58199904[-2]	0.670[-06]	-0.10	1.1	22	0.130	-1	1	10	0.39
						1	5	9	0.14
						1	7	9	0.16
-0.56829069[-2]	0.218[-17]	-9.0	0.30	-29	-0.163	-9	9	11	0.71
						-8	8	11	0.13
-0.56068974[-2]	0.715[-06]	1.7	0.43	-50	-0.278	1	1	10	0.24
						2	2	9	0.40
						2	6	9	0.13
-0.55892381[-2]	0.842[-19]	-8.0	0.15	-27	-0.153	-8	10	11	0.86
-0.53284143[-2]	0.489[-15]	-7.0	0.27	-25	-0.132	-7	9	11	0.73
						-6	8	11	0.12
-0.52057438[-2]	0.653[-14]	-6.0	0.13	-23	-0.122	-6	10	11	0.85
-0.51411343[-2]	0.542[-12]	-6.9	0.59	-24	-0.126	-8	8	11	0.12
						-7	7	11	0.48
						-6	6	11	0.21
-0.50731864[-2]	0.153[-12]	-6.0	0.40	-22	-0.114	-6	8	11	0.60
						-5	7	11	0.15
-0.49660071[-2]	0.941[-14]	-5.0	0.24	-20	-0.100	-5	9	11	0.70
-0.48800533[-2]	0.137[-08]	-5.9	0.94	-22	-0.108	-7	7	11	0.15
						-6	6	11	0.39
						-5	5	11	0.23
-0.45237511[-2]	0.399[-06]	-0.42	1.4	23	0.102	-1	1	11	0.37
						1	5	10	0.11
-0.43318751[-2]	0.410[-06]	1.2	1.5	-64	-0.276	1	1	11	0.25
						2	2	10	0.33

TABLE IV. Na atom, odd  $\pi_z$  parity, large  $d_s$  states, exciting from  $3S$  with laser polarization along **B**. See Table I caption for details.

$W$	$f$	$\langle l_z \rangle$	$D(l_z)$	$\langle x \rangle$	$d_s$	$m$	$l$	$n$	$w$
-0.75789761[-2]	0.927[-06]	0.91	0.17	-20	-0.151	1	2	8	0.58
						1	4	8	0.19
-0.75379361[-2]	0.946[-16]	-7.0	0.07	-15	-0.116	-7	8	9	0.94
-0.73890108[-2]	0.552[-05]	0.39	0.51	17	0.125	0	1	9	0.63
						1	2	8	0.15
-0.65143397[-2]	0.218[-20]	-7.9	0.10	-22	-0.141	-8	9	10	0.91
-0.62565099[-2]	0.119[-17]	-6.9	0.22	-20	-0.123	-7	8	10	0.79
						-6	7	10	0.11
-0.61247832[-2]	0.187[-18]	-6.0	0.08	-18	-0.111	-6	9	10	0.90
-0.60040828[-2]	0.304[-14]	-5.9	0.34	-18	-0.106	-6	7	10	0.67
						-5	6	10	0.15
-0.57774926[-2]	0.672[-20]	-9.0	0.15	-29	-0.168	-9	10	11	0.85
-0.55068141[-2]	0.224[-18]	-8.0	0.29	-27	-0.148	-8	9	11	0.72
						-7	8	11	0.12
-0.53985976[-2]	0.294[-17]	-7.0	0.14	-25	-0.137	-7	10	11	0.86
-0.52421835[-2]	0.850[-16]	-6.9	0.42	-25	-0.129	-7	8	11	0.60
						-6	7	11	0.17
-0.52293729[-2]	0.975[-22]	-10	0.26	-38	-0.196	-10	11	12	0.75
-0.51480155[-2]	0.789[-15]	-6.0	0.26	-23	-0.117	-6	9	11	0.73
						-5	8	11	0.11
-0.50109543[-2]	0.954[-15]	-5.0	0.12	-21	-0.106	-5	10	11	0.83
-0.49837608[-2]	0.125[-14]	-5.9	0.56	-22	-0.111	-7	8	11	0.12
						-6	7	11	0.49
						-5	6	11	0.20

believed to be due to ‘‘accidental degeneracy.’’ That is, when a state of high  $|\langle l_z \rangle|$ , which usually has very low oscillator strength, happens to be energetically close to a state of low  $|\langle l_z \rangle|$ , i.e., a case of accidental degeneracy in the energy anticrossing area, the excitation probability of this otherwise high  $|\langle l_z \rangle|$  state is expected to have considerable components of both high and low  $|\langle l_z \rangle|$  states and hence its optical excitation probability is much larger than that of a high  $|\langle l_z \rangle|$  state elsewhere [5].

No such accidental degeneracy is found in our calculations, but some states, like the third from the last in Table III

and the corresponding state of H (the last state in Table I), have stronger interactions with optically excitable states, with a  $p$ -state components of about  $0.37 \times 10^{-3}$  and  $0.17 \times 10^{-5}$ , respectively and the transition probabilities are several order of magnitude larger than those of other large  $d_s$  states.

The energy range of the observed large  $d_s$  is around  $-118 \text{ cm}^{-1}$  [5], where the energy level density is higher and ‘‘accidental degeneracy’’ is more likely to appear than in the range of Fig. 1.

However, the chance of the appearance of ‘‘accidental

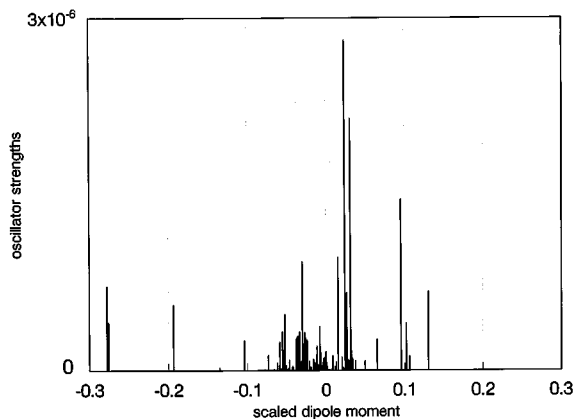


FIG. 1. Signal strength vs  $d_s$  of Na, excited from  $3S$  to high excited states with laser polarization parallel to **E**. The energy range of the states included is  $(-2040, -700) \text{ cm}^{-1}$ .

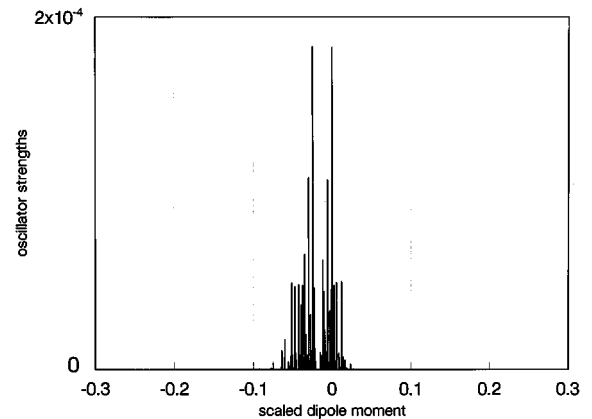


FIG. 2. Signal strength vs  $d_s$  of H, excited from  $1S$  to high excited states with laser polarization and energy range the same as Fig. 1.

degeneracy'' will still be small. If the experiment is on hydrogen, we will see that accidental degeneracies, if any, will considerably increase the signal strengths of large  $d_s$  states because these states usually have small optical excitation probabilities in the absence of accidental degeneracy.

When the experiment is on nonhydrogen atoms, we tend to consider the observed large  $d_s$  states as mainly due to those more optically excitable low  $|\langle l_z \rangle|$  states, although we cannot exclude the chance of their being due to accidental degeneracies. This is because (1) the probability of accidental degeneracy is small; (2) as the optical excitable low- $l$  components will still be smaller than that of nonhydrogen large  $d_s$  states, the transition probability to these states will be smaller compared to nonhydrogen large  $d_s$  states; (3) the calculated results have shown that a nonhydrogen low  $|\langle l_z \rangle|$  state possesses large  $d_s$  character, when it is accidentally degenerate with a high  $|\langle l_z \rangle|$  state, its  $d_s$  will not change much. In summary, the experimental signal strengths of large  $d_s$  states will not be sensitively affected by ''accidental degeneracy.''

#### IV. CONCLUSION

From the previous discussions we come to the following conclusions. (1) In the case of Coulomb plus crossed electric

and magnetic fields potential, there exist large  $d_s$  states when  $\epsilon < 0.1$ , these states have large  $|\langle l_z \rangle|$  values. (2) In nonhydrogen atoms, there exist small  $|\langle l_z \rangle|$ , large  $d_s$  states that should be considered as the effect of further symmetry breaking by the atomic core. These states are polarized along both  $\pm \mathbf{E}$  directions. The physical characteristics of these interesting states are to be further studied. (3) The experimentally observed large  $d_s$  states should mainly be nonhydrogen states. Experimental detection of these states polarized along both  $\pm \mathbf{E}$  direction would test our calculations.

Another important nonhydrogen characteristic, which has not been considered in our calculation, is the fine-structure interaction, which has considerable influence on the Rb atom. With the fine-structure term included in the Hamiltonian, the number of eigenvectors is  $\Sigma 2n^2$ ; more time and larger computer memory are needed for such calculations. This work is now under way.

#### ACKNOWLEDGMENT

This work was supported by the National Natural Science Foundation of China.

- 
- [1] C. W. Clark, E. Kroevaar, and M. G. Littman, Phys. Rev. Lett. **54**, 320 (1985).
  - [2] C. Nessmnn and P. Peinhardt, Phys. Rev. A **35**, 3269 (1987).
  - [3] M. Fauth, H. Walther, and E. Werner, Z. Phys. D **7**, 293 (1987).
  - [4] G. Wiebush, J. Main, K. Kruger, H. Rottke, A. Holle, and H. Welge, Phys. Rev. Lett. **24**, 2821 (1989).
  - [5] G. Raithel and M. Fauth, J. Phys. B **28**, 1687 (1995).
  - [6] P. F. O'Mahony, Phys. Rev. Lett. **63**, 2653 (1989).
  - [7] X. H. He, B. W. Li, A. Q. Chen, and C. X. Zhang, J. Phys. B **23**, 661 (1990).